Existence of a novel clathrin-independent endocytic pathway in yeast that depends on Rho1 and formin

Derek C. Prosser, Theodore G. Drivas, Lymarie Maldonado-Báez, and Beverly Wendland

Department of Biology, The Johns Hopkins University, Baltimore, MD 21218

Yeast is a powerful model organism for dissecting the temporal stages and choreography of the complex protein machinery during endocytosis. The only known mechanism for endocytosis in yeast is clathrin-mediated endocytosis, even though clathrin-independent endocytic pathways have been described in other eukaryotes. Here, we provide evidence for a clathrin-independent endocytic pathway in yeast. In cells lacking the clathrin-binding adaptor proteins Ent1, Ent2, Yap1801, and Yap1802, we identify a second endocytic pathway that depends on the GTPase Rho1, the downstream formin Bni1, and the Bni1 cofactors Bud6 and Spa2. This second pathway does not require components of the better-studied endocytic pathway, including clathrin and Arp2/3 complex activators. Thus, our results reveal the existence of a second pathway for endocytosis in yeast, which suggests similarities with the RhoA-dependent endocytic pathways of mammalian cells.

Introduction

Endocytosis is an evolutionarily conserved process in eukaryotes that is critical for nutrient uptake, protein and membrane turnover, and responses to the extracellular environment. To date, clathrin-mediated endocytosis (CME) is the best-studied mode of internalization from the plasma membrane, and requires the ordered recruitment of clathrin, cargo- and clathrin-binding adaptor proteins, and numerous accessory proteins. Many proteins involved in CME have been identified and characterized in yeast, most of which have orthologues in mammalian cells that perform similar functions (Engqvist-Goldstein and Drubin, 2003; Kaksonen et al., 2005; Kaksonen et al., 2006; Robertson et al., 2009); the high level of conservation highlights the fundamental role of CME in cellular function.

Although the importance of CME is well established, most cells also use clathrin-independent pathways (Mayor and Pagano, 2007; Howes et al., 2010). For example, clathrin-independent endocytosis (CIE) in mammalian cells occurs through caveolae (Kiss and Botos, 2009), phagocytosis, macropinocytosis, and the clathrin- and dynamin-independent carrier/glycosylphosphatidylinositol-anchored protein-enriched early endosomal compartment (CLIC–GEEC) pathway (Sabharanjak et al., 2002). There are other clathrin-independent mechanisms that use Rho and Arf family GTPases (Radhakrishna and Donaldson, 1997; Lamaze et al., 2001). The variety of CIE mechanisms may have arisen to satisfy the specific needs of different cell types by permitting internalization of specific cargos or by activating endocytosis in response to environmental or stress conditions.

Because multiple endocytic pathways have been identified in most eukaryotes, it is perhaps surprising that only CME has been described to date in any fungal species. However, previous findings suggest the existence of CIE mechanisms: endocytosis proceeds, albeit at reduced rates, in clathrin-null cells (Payne et al., 1988; Chu et al., 1996; Kaksonen et al., 2005; Newpher and Lemmon, 2006), and deletion or mutation of other genes required for CME, such as *LAS17*, severely reduce but do not abolish endocytosis (Madania et al., 1999). One interpretation of these findings is that residual activity of CME machinery in the absence of clathrin allows membrane internalization, although it is unclear whether cargo proteins are recruited to putative residual CME sites (Kaksonen et al., 2005; Newpher and Lemmon, 2006). An alternative but not mutually exclusive interpretation is that unrecognized CIE mechanisms exist

Correspondence to Beverly Wendland: bwendland@jhu.edu

Lymarie Maldonado-Báez's present address is Laboratory of Cell Biology, National Heart, Lung and Blood Institute, National Institutes of Health, Bethesda, MD 20892.

Abbreviations used in this paper: 5-FAA, 5-fluoroanthranilic acid; a.u., arbitrary units; CIE, clathrin-independent endocytosis; CME, clathrin-mediated endocytosis; CWI, cell wall integrity; DAD, diaphanous autoregulatory domain; ENTH, epsin N-terminal homology; LatA, Latrunculin A; WT, wild type; YNB, yeast nitrogen base; YPD, yeast peptone dextrose.

The Rockefeller University Press $30.00
J. Cell Biol. Vol. 195 No. 4 657–671
www.jcb.org/cgi/doi/10.1083/jcb.201104045

in yeast, which might act with or parallel to the known CME machinery or its residual components in CME mutants.

We recently characterized the role of endocytic adaptor proteins in the budding yeast *Saccharomyces cerevisiae* (Aguilar et al., 2006; Maldonado-Báez et al., 2008). The yeast genome encodes four monomeric adaptors that perform genetically overlapping functions: the epsins Ent1 and Ent2 and the AP180/CALM homologues Yap1801 and Yap1802. These adaptor proteins bind phosphatidylinositol (4,5)-bisphosphate via an epsin or AP180 N-terminal homology domain (epsin N-terminal homology [ENTH] or ANTH, respectively), clathrin through a C-terminal clathrin-binding motif, and cargo and endocytic accessory proteins (Aguilar et al., 2003). Although *ENT1* and *ENT2* are an essential gene pair, the ENTH domain of either protein is sufficient for viability and regulates Cdc42, a GTPase that controls polarity (Wendland et al., 1999; Aguilar et al., 2006). *ent1*Δ *ent2*Δ+ENTH1 (ENTH1; Ent1 ENTH domain) cells are viable and competent for endocytosis, whereas *ent1*Δ *ent2*Δ *yap1801*Δ *yap1802*Δ+ENTH1 (4Δ+ENTH1) cells show delayed endocytosis, are temperature-sensitive for growth, and have aberrant behavior of CME machinery at cortical patches (Maldonado-Báez et al., 2008). Endocytosis and growth defects of 4Δ+ENTH1 cells are corrected by reintroducing any one of the four full-length adaptors, so long as an ENTH domain is present to maintain viability.

To identify proteins that promote endocytosis in the absence of monomeric adaptors, we performed a high-copy suppressor screen in 4Δ+ENTH1 cells, where CME pathway function is greatly reduced, to find genes that restored temperature-dependent growth and endocytosis. We show that components of the Rho1-dependent cell wall integrity (CWI)-sensing pathway mediate an endocytic route that requires one of the two formins, Bni1 (but not Bnr1), and polarity determinants that interact with Bni1. Rho1-dependent endocytosis does not require clathrin, robust Arp2/3-mediated actin polymerization, or key actin-binding proteins known to promote CME at endocytic patches. 4Δ+ENTH1 growth and endocytosis defects are suppressed by the Rho1 pathway, yet the suppressed cells still exhibit aberrant dynamics of the known CME machinery. These findings are consistent with the existence of a CIE pathway that depends upon Rho1.

Results

Mid2, Rom1, and Rho1 promote endocytosis in adaptor-null cells

We showed previously that yeast cells lacking the endocytic adaptors *ENT1*, *ENT2*, *YAP1801*, and *YAP1802* have a pronounced defect in endocytosis and are temperature-sensitive for growth. To identify genes that suppress the growth and endocytic defects of 4Δ+ENTH1 cells, we first screened a high-copy yeast genomic DNA library for plasmids that allowed growth at 37°C. Three candidate genes isolated from this screen act in a signaling cascade that includes the CWI pathway: the cell wall stress sensor Mid2, the Rho1 guanine nucleotide exchange factor (GEF) Rom1, and the GTPase Rho1 (Fig. 1 A). Upon cell wall damage, Mid2 is thought to recruit Rom1 and the related GEF Rom2 to the plasma membrane to locally activate Rho1 (Philip and Levin, 2001). Active GTP-bound Rho1 then binds to effector proteins that mediate cell wall repair and actin repolarization (Delley and Hall, 1999).

4Δ+ENTH1 cells are inviable at 37°C, and the suppressor plasmids only weakly supported growth at this temperature (unpublished data). In contrast, 4Δ+ENTH1 cells grew poorly at 35.5°C compared with wild-type (WT) or 4Δ cells complemented with full-length Ent1 (4Δ+Ent1; Fig. 1 B). Multicopy Mid2, Rom1, and Rho1 in 4Δ+ENTH1 cells exhibited improved growth at 35.5°C. High-copy expression of the clathrin-binding adaptor Yap1801 also allowed growth of 4Δ+ENTH1 cells at 35.5°C, as we found previously (Maldonado-Báez et al., 2008). Multicopy expression of the cell wall stress sensor Wsc1, which also signals to Rho1 via Rom1/2 (Philip and Levin, 2001), did not promote growth of 4Δ+ENTH1 at 35.5°C. All strains grew similarly at 30°C (Fig. 1 B). The suppressor and *YAP1801* plasmids did not bypass the essential requirement for the ENTH domain because none of the 4Δ cells with suppressor plasmids only grew on 5-fluoroanthranilic acid (5-FAA), which selects for loss of Ent1 or ENTH1 [*CEN TRP1*] plasmids (Fig. S1). Single or multicopy Ent1 or HA-ENTH1 on a *URA3*-containing plasmid permitted growth of 4Δ+ENTH1 [*CEN TRP1*] cells on 5-FAA (Aguilar et al., 2006), which indicates that 4Δ cells expressing an ENTH domain protein are not 5-FAA sensitive. Thus, multicopy expression of Rho1 pathway components suppressed the growth defect of 4Δ+ENTH1 cells.

We next asked if the Rho1 pathway could promote endocytosis in 4Δ+ENTH1 cells using the a-factor pheromone receptor Ste3, which undergoes constitutive endocytosis and targeting to the vacuole (Shaw et al., 2003). As expected, steady-state localization of Ste3-GFP was primarily vacuolar in WT and 4Δ+Ent1 cells, with little fluorescent signal at the plasma membrane (Fig. 1 C; Maldonado-Báez et al., 2008). In contrast, 4Δ+ENTH1 cells accumulated a pool of Ste3-GFP at the plasma membrane, which is consistent with defective endocytosis, although some vacuolar Ste3-GFP remained. Like the suppression of temperature-sensitive growth, high-copy Mid2, Rom1, or Rho1, as well as Yap1801, partially restored Ste3-GFP internalization, whereas Wsc1 resembled empty vector. Rom2 also promoted Ste3-GFP internalization in 4Δ+ENTH1 cells, whereas high-copy Rho2-Rho5 and Cdc42 did not (unpublished data). These data demonstrate that suppression of endocytic defects is specific to Mid2, Rom1/Rom2, and Rho1, and is not mediated by Wsc1 or other Rho-family GTPases.

We recently showed that steady-state cargo outside of the multivesicular body/vacuole can be quantified using Ste3 tagged with super-ecliptic pHluorin, a pH-sensitive GFP variant (Miesenböck et al., 1998; Sankaranarayanan et al., 2000; Prosser et al., 2010). Using this approach, 4Δ+ENTH1 cells had significantly brighter Ste3-pHluorin fluorescence levels than WT or 4Δ+Ent1 cells (Prosser et al., 2010). As expected, 4Δ+ENTH1 cells with either empty vector or Wsc1 had significantly brighter Ste3-pHluorin fluorescence than WT cells. High-copy Yap1801, Mid2, Rom1, or Rho1 reduced the fluorescence

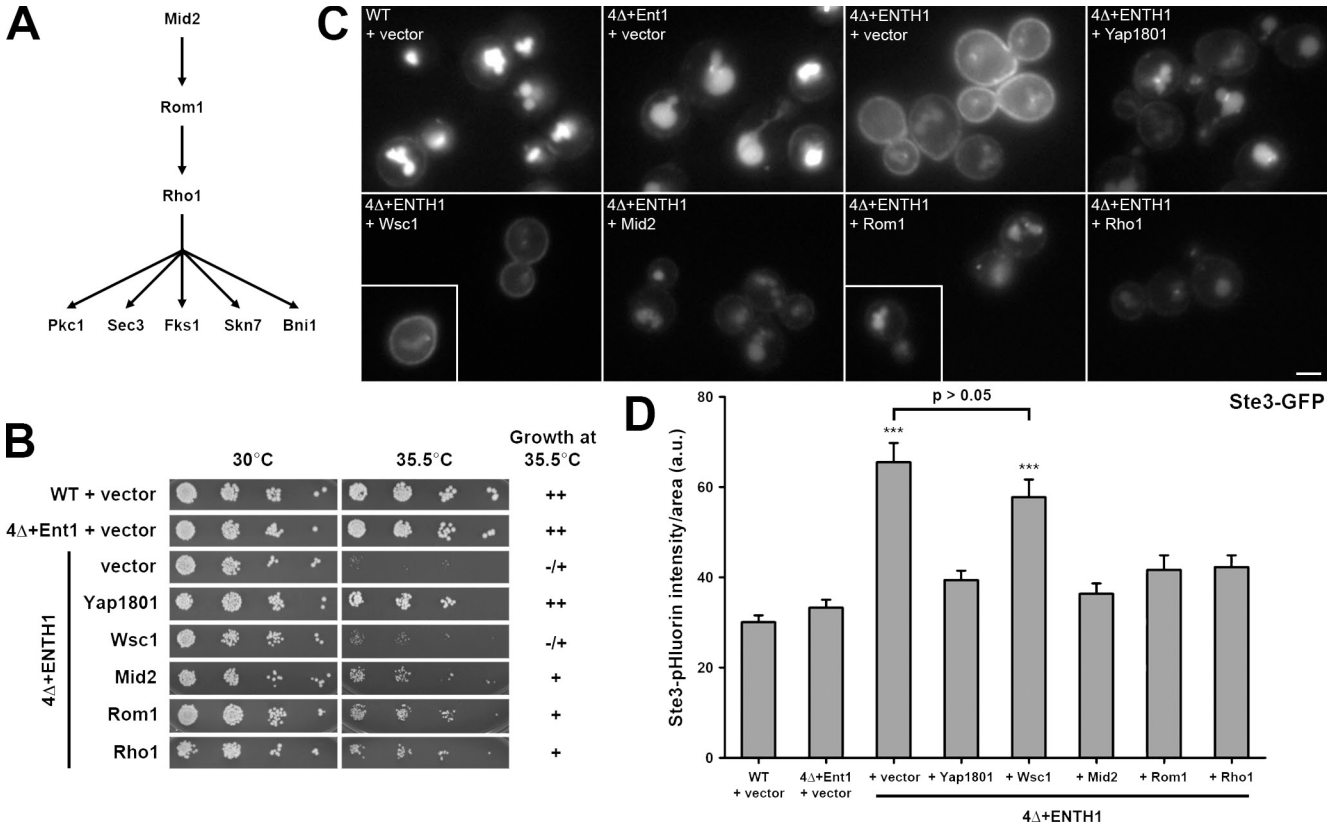

Figure 1. **Suppression of temperature-dependent growth and endocytic defects by the Rho1 pathway.** (A) Schematic of Rho1 pathway components. (B) Five-fold serial dilutions of WT, 4Δ+Ent1, and 4Δ+ENTH1 cells with empty vector, *YAP1801*, *WSC1*, *MID2*, *ROM1*, and *RHO1* plasmids as indicated were grown at 30°C or 35.5°C. Growth at 35.5°C was scored as strong (++), moderate (+), or weak (−/+). (C) Cells from B, which express Ste3-GFP at endogenous levels, were examined by fluorescence microscopy. Insets show additional cells at the same magnification. Bar, 2.5 µm. (D) Intensity of Ste3-pHluorin was quantified in WT, 4Δ+Ent1, and 4Δ+ENTH1 cells expressing Ste3-pHluorin with the same plasmids used in B. Intensity values corrected for cell size are expressed in arbitrary units (a.u.; error bars indicate mean ± SEM; ***, $P < 0.001$ compared with all other conditions).

levels of 4Δ+ENTH1 cells toward those of WT and 4Δ+Ent1 cells (Fig. 1 D), which indicates that the Rho1 pathway suppresses the endocytic defect of 4Δ+ENTH1 cells. For all experiments in this study, Mid2, Rom1, and Rho1 behaved similarly; for brevity, we used Rom1 as a representative suppressor within the Rho1 pathway.

Endocytosis through the Rho1 pathway is not cargo selective in adaptor mutant cells

To determine whether endocytosis through the Rho1 pathway is specific to Ste3, we assessed endocytosis of the methionine permease Mup1, which is internalized rapidly upon exposure to methionine. As seen previously (Prosser et al., 2010), WT cells showed a 60–70% decrease in Mup1-pHluorin intensity 30 min after adding methionine (Fig. 2, A and B). Although 4Δ+Ent1 cells behaved similarly to WT, 4Δ+ENTH1 cells were significantly delayed for Mup1 internalization (10–15% decrease in Mup1-pHluorin intensity). Multicopy Rom1 partially restored methionine-dependent Mup1 internalization, resulting in a 35% decrease in Mup1-pHluorin intensity. Thus, multiple cargos undergoing either constitutive or regulated endocytosis can enter through the Rho1 pathway in 4Δ+ENTH1 cells. In addition, multicopy Rom1 promoted uptake of the fluid-phase marker Lucifer yellow in 4Δ+ENTH1 cells (unpublished data), which further suggests that Rho1-mediated endocytosis is not cargo-selective.

Endocytosis through the Rho1 pathway is actin dependent

The Rho1 pathway may localize Ste3-GFP to the vacuole via two distinct routes: by promoting endocytic events at the plasma membrane or by bypassing the plasma membrane and redirecting cell surface–destined cargos, leaving the Golgi complex to the vacuole. To distinguish between these possibilities, we treated cells with the actin-depolymerizing drug Latrunculin A (LatA), which abolishes endocytosis but does not block transport from Golgi to the plasma membrane or the vacuole (Ayscough et al., 1997; Huang and Chang, 2011). As expected, Ste3-GFP was in the vacuole in control cells treated with vehicle (DMSO) and accumulated at the plasma membrane in LatA-treated WT and 4Δ+Ent1 cells, and under both LatA and DMSO conditions in 4Δ+ENTH1 cells (Fig. 3). LatA-treated 4Δ+ENTH1 cells with multicopy Rom1 accumulated Ste3-GFP at the plasma membrane, which indicates that actin dynamics are required for endocytosis through the Rho1 pathway. Along with the Mup1-pHluorin results, these data also suggest that cargo proteins are still transported to the cell surface before being targeted to the vacuole in cells with multicopy Rom1.

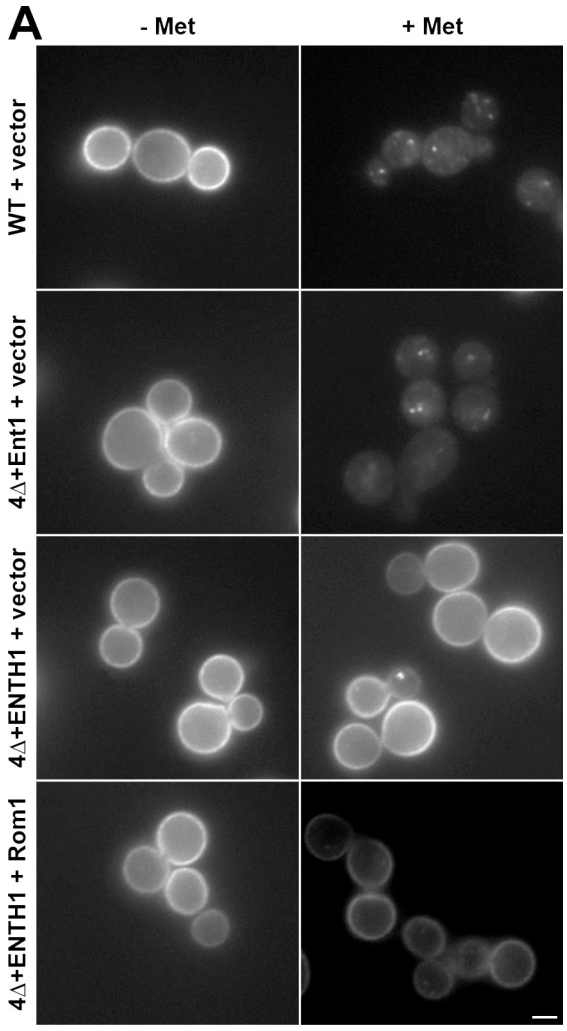

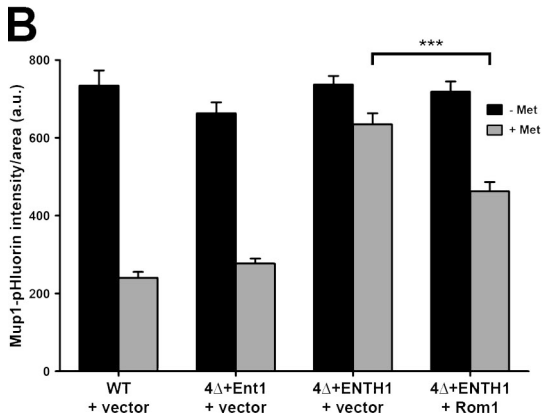

Figure 2. **Effect of multicopy Rom1 on methionine-induced internalization of Mup1-pHluorin in adaptor mutant cells.** (A) WT, 4Δ+Ent1, and 4Δ+ENTH1 cells with empty vector or Rom1 as indicated were grown in the absence of methionine to promote accumulation of Mup1 at the plasma membrane. Random fields of cells were imaged before treatment (−Met) or 30 min after addition of 20 µg/ml methionine (+Met) to the medium. For all images, identical maximum and minimum intensity values were applied to allow comparison of fluorescence intensity. Bar, 2.5 µm. (B) Quantification of Mup1-pHluorin intensity (a.u.; error bars indicate mean ± SEM; ***, $P < 0.001$) from the experiment in A. Black bars represent untreated (−Met) cells, whereas gray bars represent methionine-treated cells (+Met).

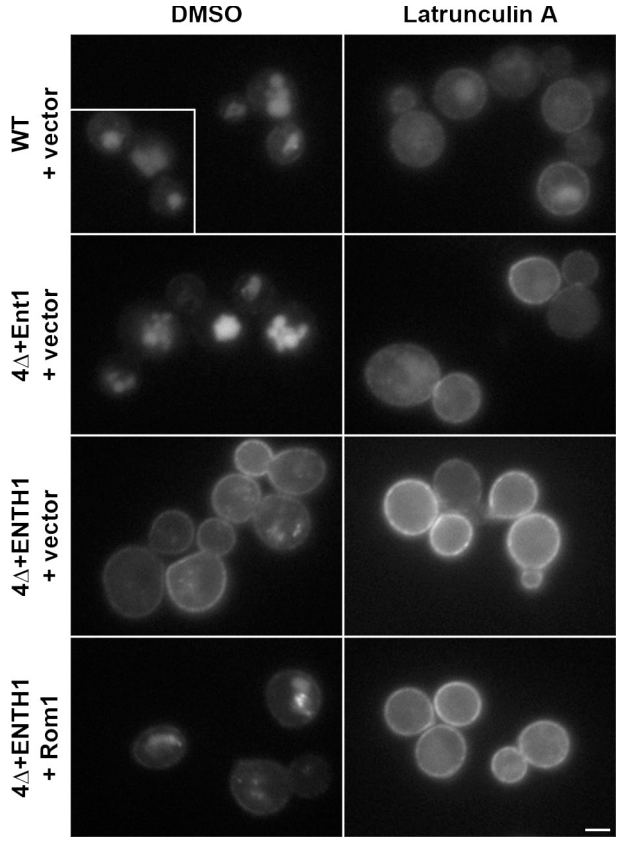

Figure 3. **The Rho1 pathway mediates actin-dependent internalization from the plasma membrane.** WT, 4Δ+Ent1, and 4Δ+ENTH1 cells with empty vector or Rom1 were treated with 200 µM LatA or an equivalent volume of DMSO for 2 h before visualization of Ste3-GFP by fluorescence microscopy. The inset shows additional cells at the same magnification. Bar, 2.5 µm.

The formin Bni1 is required downstream of the Rho1 endocytic pathway

There are five known effectors of Rho1: (1) the atypical protein kinase C Pkc1, which regulates cell wall repair via the mitogen-activated protein kinase Mpk1/Slt2; (2) the actin cable-assembling formin Bni1; (3) the transcription factor Skn7 involved in osmotic and oxidative stress responses; (4) the exocyst component Sec3 involved in polarized secretion; and (5) Fks1, the catalytic subunit of β-glucan synthase (Fig. 1 A; for review see Levin, 2005). To define how Rho1 mediates endocytosis, we deleted each Rho1 effector in 4Δ+ENTH1 cells and asked whether upstream components of the pathway still promoted endocytosis. Deleting *PKC1* causes cell lysis, whereas cells tolerate deleting the downstream kinases *BCK1* and *SLT2* (Lee and Levin, 1992; Levin and Bartlett-Heubusch, 1992; Mazzoni et al., 1993). We generated *bck1*Δ and *slt2*Δ strains in WT and 4Δ backgrounds; however, loss of either gene in 4Δ+ENTH1 led to extremely poor growth even when grown with osmotic support; we were unable to further analyze these cells (unpublished data).

Although we could not assess the role of Pkc1 and its downstream targets, we could study the effect of *bni1*Δ, *skn7*Δ, *sec3*Δ, and *fks1*Δ on Ste3-GFP localization in the WT and 4Δ backgrounds. Deleting any of these Rho1 effectors did not alter

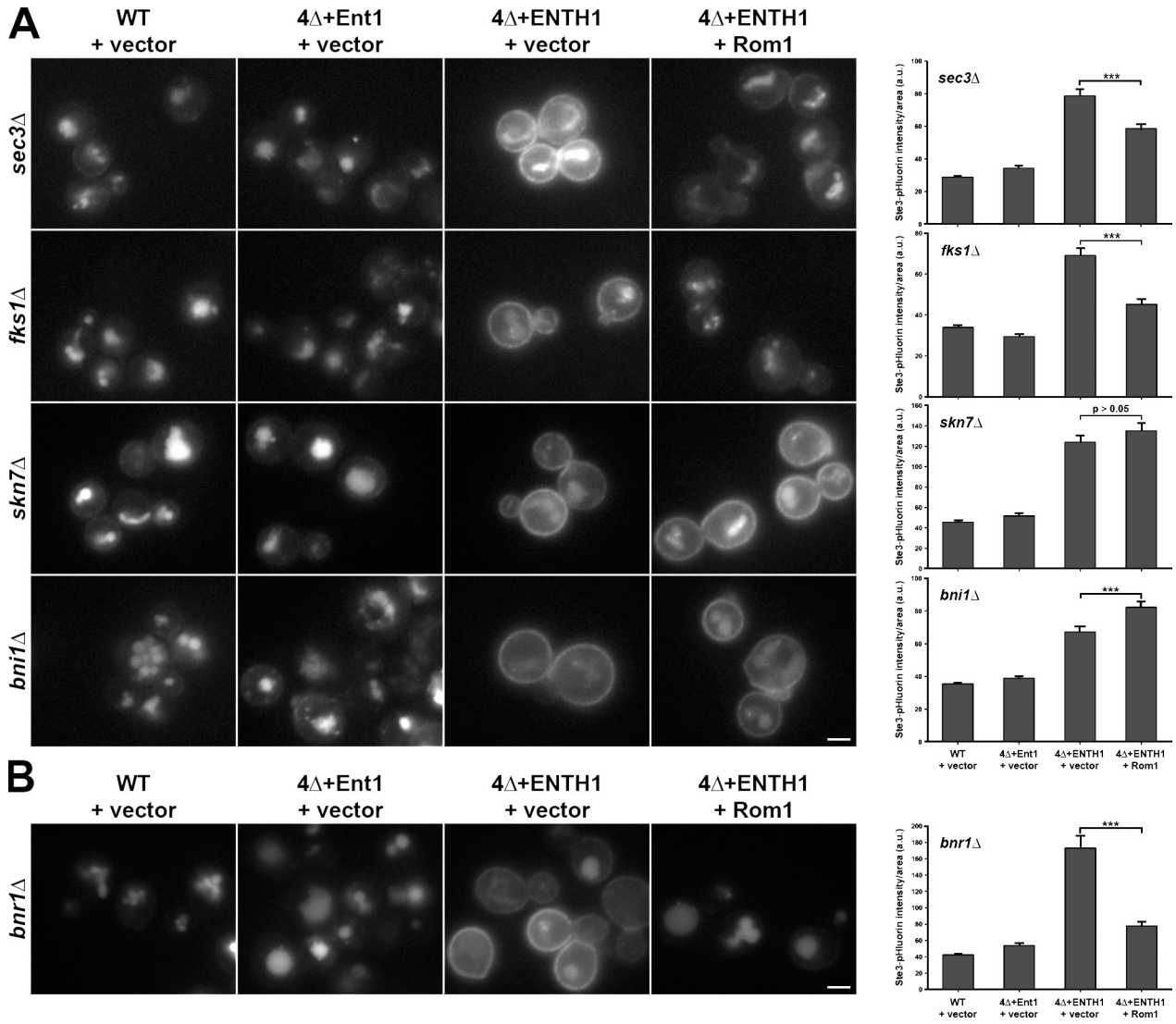

Figure 4. **Effect of Rho1 effector deletion on endocytosis mediated by the Rho1 pathway.** (A) Ste3-GFP was visualized by fluorescence microscopy in *sec3*Δ, *fks1*Δ, *skn7*Δ, and *bni1*Δ strains generated in WT, 4Δ+Ent1, and 4Δ+ENTH1 backgrounds with empty vector or Rom1 plasmids as indicated. (B) Ste3-GFP localization was assessed by fluorescence microscopy in *bnr1*Δ strains generated in WT, 4Δ+Ent1, and 4Δ+ENTH1 backgrounds with empty vector or Rom1 plasmids. Quantification of Ste3-pHluorin intensity (a.u.; error bars indicate mean ± SEM; ***, P < 0.001) is shown to the right of each group of images. Bars, 2.5 µm.

vacuole localization of Ste3-GFP in WT and 4Δ+Ent1 adaptor strains, whereas Ste3-GFP accumulated at the plasma membrane in the 4Δ+ENTH1 strains (Fig. 4 A). Neither Sec3 nor Fks1 acts downstream of the Rho1 pathway in endocytosis, as high-copy Rom1 improved Ste3-GFP internalization in *sec3*Δ or *fks1*Δ 4Δ+ENTH1 cells. In contrast, high-copy Rom1 did not promote Ste3-GFP internalization in 4Δ+ENTH1 cells lacking *SKN7* or *BNI1*. In all cases, quantification of Ste3-pHluorin intensity agreed with Ste3-GFP localization, where multicopy Rom1 significantly reduced Ste3-pHluorin intensity in *sec3*Δ or *fks1*Δ 4Δ+ENTH1 cells, but not in *skn7*Δ or *bni1*Δ 4Δ+ENTH1 cells. In fact, Rom1-expressing *bni1*Δ 4Δ+ENTH1 cells had a statistically significant increase in Ste3-pHluorin intensity compared with vector alone. We conclude that both Skn7 and Bni1 contribute to Rho1-mediated endocytosis. For the remainder of this study, we focused on analyzing the role of Bni1, as formins contribute to actin cable assembly, and actin dynamics are absolutely required for endocytosis in yeast.

As a complementary approach to deleting individual Rho1 effectors, we also asked if multicopy expression of Rho1 effectors suppressed endocytic defects in 4Δ+ENTH1 cells. Surprisingly, Ste3-GFP internalization defects were not corrected by high-copy Bni1 or Skn7 in 4Δ+ENTH1 cells; Pkc1, Sec3, and Fks1 similarly failed to suppress the endocytic defects (Fig. S2 A). Single-copy expression of constitutively active Pkc1* or multicopy expression of the downstream kinases Bck1-20 (activated Bck1), Mkk1, or Slt2 also did not improve Ste3-GFP internalization in 4Δ+ENTH1 cells. Quantification of Ste3-pHluorin intensity did not reveal a significant difference between 4Δ+ENTH1 cells with empty vector or any of the Rho1 effector plasmids (Fig. S2 B). These results suggest that

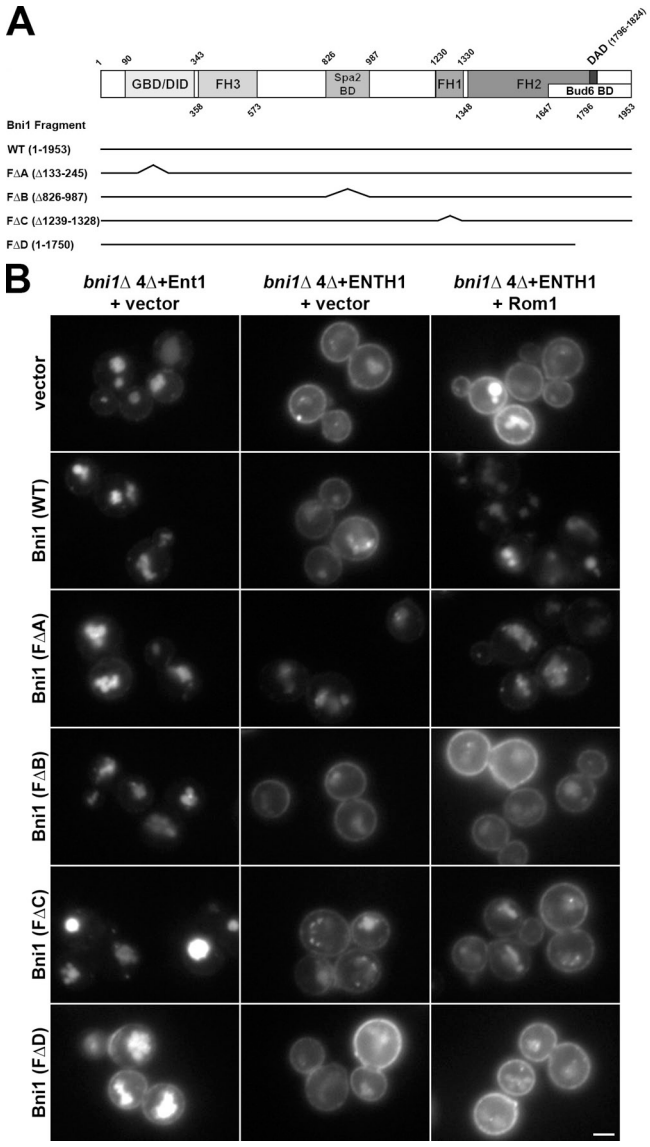

Figure 5. **Contribution of Bni1 protein–protein interaction regions to Rho1-mediated endocytosis.** (A) Schematic of full-length and truncated Bni1 fragments used. Bni1 fragments were expressed from the *BNI1* promoter. (B) Ste3-GFP was examined by fluorescence microscopy in *bni1*Δ 4Δ+Ent1 and *bni1*Δ 4Δ+ENTH1 cells with empty vector, full-length or truncated Bni1 fragments [*CEN TRP1*], and empty vector or high-copy Rom1 [2μ *URA3*] plasmids as indicated. Bar, 2.5 μm.

activation of the CWI pathway downstream of Pkc1 does not contribute to Rho1-mediated endocytosis. The unexpected lack of suppression by high-copy Bni1 may be caused by inefficient or mislocalized activation of the full-length formin (Fig. 5 B and Discussion).

Rho1-mediated endocytosis specifically requires Bni1, and not the related formin Bnr1

Because Rho1-mediated endocytosis is inhibited by actin depolymerization and Bni1 mediates actin cable nucleation and elongation, we examined the role of Bni1 as a potential mediator of endocytosis downstream of Rho1. Budding yeast express two related formins, Bni1 and Bnr1, that share partially overlapping functions; Bni1 acts downstream of Rho1 and assembles cables in the bud, whereas Bnr1 localizes to the bud neck and assembles cables that fill the mother (Pruyne et al., 2004). As seen with the uninvolved Rho1 effectors Sec3 and Fks1, high-copy Rom1 promoted Ste3-GFP internalization in *bnr1*Δ 4Δ+ENTH1 cells and reduced Ste3-pHluorin intensity (Fig. 4 B). Furthermore, multicopy Rom1 promoted methionine-dependent Mup1 internalization in *bnr1*Δ 4Δ+ENTH1 cells but not in *bni1*Δ 4Δ+ENTH1 cells, as revealed by quantification of Mup1-pHluorin intensity (Fig. S3). Thus, Bni1 is specifically required downstream of Rho1 for endocytosis, and Bnr1 is unlikely to contribute to this pathway.

Bni1 protein–protein interaction domains contribute to Rho1-mediated endocytosis

Bni1 interacts with actin-regulating factors such as profilin, the GTPases Rho1 and Cdc42, and the polarisome components Spa2 and Bud6 (Evangelista et al., 1997; Imamura et al., 1997; Fujiwara et al., 1998; Ozaki-Kuroda et al., 2001); thus, we asked whether specific protein–protein interaction regions of Bni1 contribute to Rho1-mediated endocytosis. As summarized in Fig. 5 A, Bni1 is thought to adopt an inactive state via an autoinhibitory interaction between its N-terminal diaphanous inhibitory domain (DID) and its C-terminal diaphanous autoregulatory domain (DAD; Alberts, 2001). The DAD–DID autoinhibitory interaction may be relieved upon binding of Rho1-GTP to the N-terminal GTPase-binding domain (GBD), or by other stimulatory cues, resulting in localized Bni1 activation at the bud cortex (Evangelista et al., 2002). Maximal actin cable assembly by Bni1 requires its DAD-binding ligand Bud6, which recruits actin monomers to enhance Bni1 nucleation activity (Moseley et al., 2004). The formin homology 1 (FH1) domain binds profilin directly to mediate FH2 domain-dependent incorporation of actin-ATP monomers onto the barbed end of unbranched actin filaments (Imamura et al., 1997). Finally, Spa2 binds to Bni1 at a distinct site to recruit Bni1 to the bud tip (Fujiwara et al., 1998).

We expressed truncated Bni1 fragments lacking the GBD, Spa2-binding region, FH1 domain, or DAD/Bud6-binding region, referred to as FΔA, FΔB, FΔC, and FΔD, respectively (Ozaki-Kuroda et al., 2001), and asked if these fragments supported Rho1-mediated endocytosis. Each fragment was expressed from a single-copy plasmid as the sole source of Bni1 in *bni1*Δ 4Δ cells. Interestingly, the FΔA fragment partially restored Ste3-GFP internalization in *bni1*Δ 4Δ+ENTH1 transformed with empty vector, whereas full-length Bni1 and the FΔB, FΔC, and FΔD fragments did not (Fig. 5 B). Further, expression of FΔD had a mildly deleterious effect on Ste3-GFP internalization in *bni1*Δ 4Δ+Ent1 cells, which showed no obvious defect in endocytosis with empty vector or the other fragments. High-copy Rom1 improved endocytosis in *bni1*Δ 4Δ+ENTH1 cells expressing full-length Bni1 but not FΔB, FΔC, and FΔD, and Rom1 did not further increase endocytosis in FΔA-expressing cells (Fig. 5 B). Thus, FΔA is likely able to bypass the requirement for Rho1 pathway overexpression, whereas both catalytic activity and interaction with the polarisome are necessary for Bni1 to mediate endocytosis.

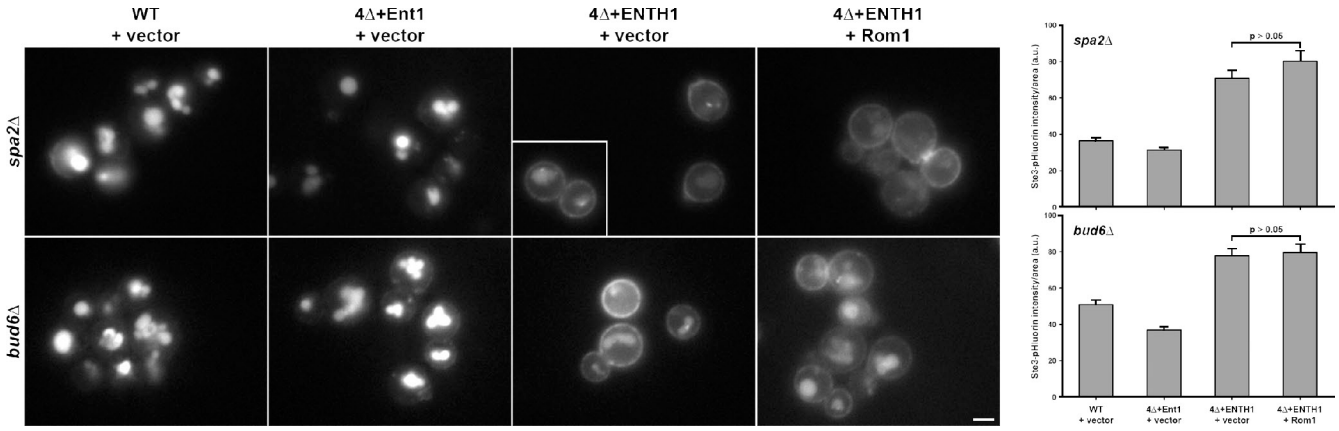

Figure 6. **Requirement of polarisome components for Rho1-mediated endocytosis.** *spa2*Δ and *bud6*Δ strains were generated in WT, 4Δ+Ent1, and 4Δ+ENTH1 backgrounds with empty vector or Rom1 plasmids as indicated. Ste3-GFP localization was assessed by fluorescence microscopy. Quantification of Ste3-pHluorin intensity (a.u.; error bars indicate mean ± SEM) is shown to the right of each group of Ste3-GFP images. The inset shows additional cells at the same magnification. Bar, 2.5 µm.

Components of the polarisome are required for Rho1-mediated endocytosis

The polarisome is a seven-subunit protein complex in yeast that acts as a scaffold for regulating polarity and directing cargo delivery along actin cables to the tips of growing buds and mating projections (Sheu et al., 1998). Spa2 and Bud6 are two polarisome proteins that physically interact with Bni1; data from *spa2*Δ and *bud6*Δ cells suggest that these proteins promote Bni1 actin assembly activity (Fujiwara et al., 1998; Ozaki-Kuroda et al., 2001). Consistent with the Bni1 truncation experiments above, high-copy Rom1 did not promote endocytosis in *bud6*Δ or *spa2*Δ 4Δ+ENTH1 cells, and did not reduce Ste3-pHluorin intensity compared with empty vector (Fig. 6). Ste3-GFP localization was unaffected when *SPA2* or *BUD6* were deleted in a WT or 4Δ+Ent1 background. Thus, Bni1-interacting polarisome subunits are required for Rho1-mediated endocytosis.

Actin cables, and not cortical patches, are required for endocytosis through the Rho1 pathway

Bni1 has not previously been implicated in endocytosis at (or localization to) cortical patches, and its activity is thought to be restricted to actin cables (Sagot et al., 2002; deHart et al., 2003). Because the Rho1 pathway requires Bni1, we reasoned that this pathway should depend on actin cables, and not on cortical actin patches where CME occurs. Actin polymerization and stabilization are regulated by distinct mechanisms at cortical patches versus cables; thus, we asked if patch- and/or cable-specific regulatory factors are required for the Rho1 pathway.

First, we tested cells lacking *LAS17*, the yeast Wiskott-Aldrich syndrome protein orthologue and major activator of Arp2/3-mediated actin polymerization (Sun et al., 2006). *las17*Δ cells have severe endocytic defects and highly aberrant cortical patch dynamics, with greatly extended patch lifetimes and little to no inward movement of patch proteins; these behaviors are indicative of nonfunctional endocytic sites that do not invaginate to form an endocytic vesicle (Madania et al., 1999; Sun et al., 2006). As expected, Ste3-GFP was retained at the plasma membrane in *las17*Δ cells (Fig. 7 A). High-copy Rom1 improved Ste3-GFP internalization, whereas high-copy Yap1801, which suppressed the endocytic defect in 4Δ+ENTH1 cells, did not restore Ste3 internalization in *las17*Δ cells. Similarly, high-copy Rom1 significantly reduced Ste3-pHluorin intensity in *las17*Δ cells, whereas Yap1801 did not. Thus, the Rho1 pathway appears to be independent of Arp2/3 activation by its primary nucleation-promoting factor Las17.

We then tested the requirement for a stable branched actin network at cortical patches using cells lacking *SAC6*/fimbrin and *SCP1*/transgelin. Although actin polymerization at cortical patches occurs in *sac6*Δ *scp1*Δ cells, these cortical structures fail to internalize, possibly because of defects in force generation (Goodman et al., 2003; Winder et al., 2003; Aghamohammadzadeh and Ayscough, 2009). As in *las17*Δ cells, Ste3-GFP was largely retained at the plasma membrane in *sac6*Δ *scp1*Δ cells; high-copy Rom1 promoted Ste3-GFP internalization and reduced Ste3-pHluorin intensity compared with empty vector (Fig. 7 B). In *sac6*Δ *scp1*Δ cells, multicopy Yap1801 slightly improved Ste3-GFP internalization and reduced Ste3-pHluorin intensity levels; however, Yap1801 was less effective than Rom1 in promoting Ste3 internalization. These data indicate that stability of actin at cortical patches is not required for the Rho1 pathway.

We next asked if stabilization of actin cables is required for Rho1-mediated endocytosis by testing Tpm1, which binds to the sides of unbranched actin filaments assembled by formins (Liu and Bretscher, 1989; Drees et al., 1995). *S. cerevisiae* has a second tropomyosin isoform, Tpm2, but deletion of *TPM1* alone abolishes most detectable actin cables (*tpm2*Δ has only a mild effect, if any), which indicates that Tpm1 is the primary stabilizer of actin cables. Notably, *TPM2* was also identified as a high-copy suppressor in our initial screen (unpublished data). Ste3-GFP localization in *tpm1*Δ and *tpm1*Δ 4Δ+Ent1 cells was indistinguishable from WT, whereas *tpm1*Δ 4Δ+ENTH1 cells showed plasma membrane Ste3-GFP distribution and Ste3-pHluorin intensity that were not corrected with high-copy

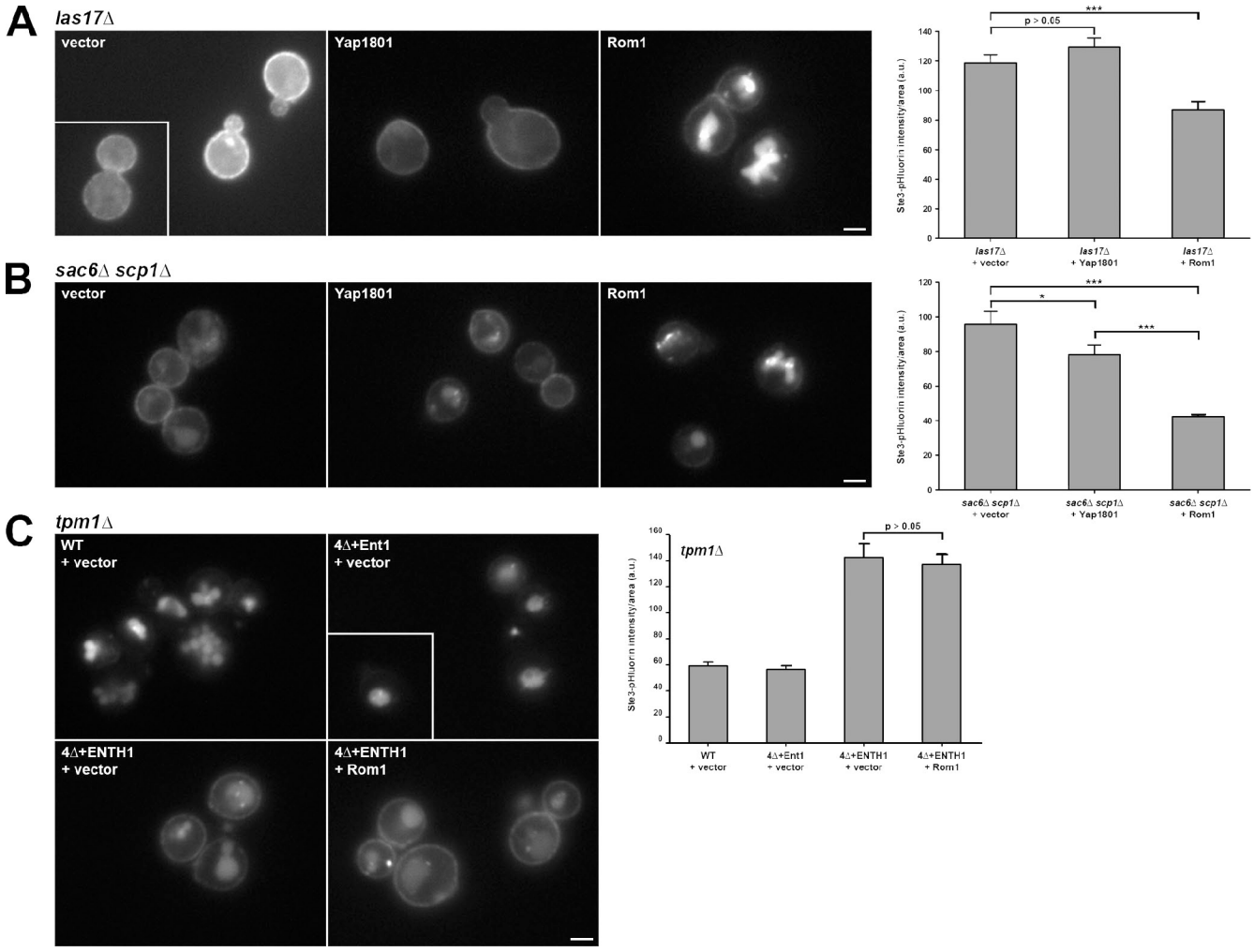

Figure 7. **Requirement of actin cable stabilization, but not actin polymerization or stabilization at cortical patches, for Rho1-mediated endocytosis.** (A and B) Ste3-GFP localization was assessed in *las17*Δ (A) and *sac6*Δ *scp1*Δ (B) cells with empty vector, Yap1801, or Rom1 plasmids. (C) *tpm1*Δ was generated in WT, 4Δ+Ent1, and 4Δ+ENTH1 cells, and Ste3-GFP localization was assessed in strains with empty vector or Rom1 as indicated. Quantification of Ste3-pHluorin intensity (a.u.; error bars indicate mean ± SEM; *, P < 0.05; ***, P < 0.001) is shown to the right of each group of Ste3-GFP images. Insets show additional cells at the same magnification. Bars, 2.5 µm.

Rom1 (Fig. 7 C). Thus, stable actin cables are required for the Rho1 pathway, whereas stability of actin at cortical patches appears to be dispensable. These results also demonstrate that the Rho1 pathway suppresses defects in multiple CME mutant backgrounds, and not only in 4Δ+ENTH1 cells.

Adaptor mutant cells develop abnormal cortical structures that are not corrected by the Rho1 pathway

Abnormal cortical patches are commonly found in strains lacking key CME machinery components. For example, dysregulated actin polymerization is seen in *chc1*Δ and *sla2*Δ cells, in which the actin-binding protein Abp1 localizes to elongated comet tail structures instead of at discrete cortical patches seen in WT cells (Kaksonen et al., 2005; Newpher and Lemmon, 2006). We assessed Abp1 localization in our cells, and observed discrete Abp1-mCherry cortical patches in WT and 4Δ+Ent1 cells (Fig. 8, A and B). These patches exhibited the expected colocalization with the late coat component Sla1, the actin nucleation-promoting factor Las17, and the actin module proteins Sac6, Rvs167/amphiphysin, and Sjl2/synaptojanin. In contrast, 4Δ+ENTH1 cells had fewer, abnormally bright Abp1 comet tail structures. These Abp1-mCherry comet tails formed from cortical foci labeled with Sla1-GFP and Las17-GFP, and also contained GFP-tagged Sac6, Rvs167, and Sjl2, which indicates that multiple cortical patch components that arrive during actin assembly are recruited to the length of the comet tails. High-copy Rom1 did not reduce Abp1 comet tails, even though it restored Ste3-GFP endocytosis (Figs. 1 C and 8 B).

The Rho1 pathway does not restore cortical patch dynamics in adaptor mutant cells

We wanted to determine if the Rho1 pathway acts through cortical patches (sites of CME in yeast) or other plasma membrane sites. We monitored the lifetime and dynamics of cortical patch proteins, including the early coat component Ede1, the late coat component Pan1, and the actin nucleation-promoting factor Las17

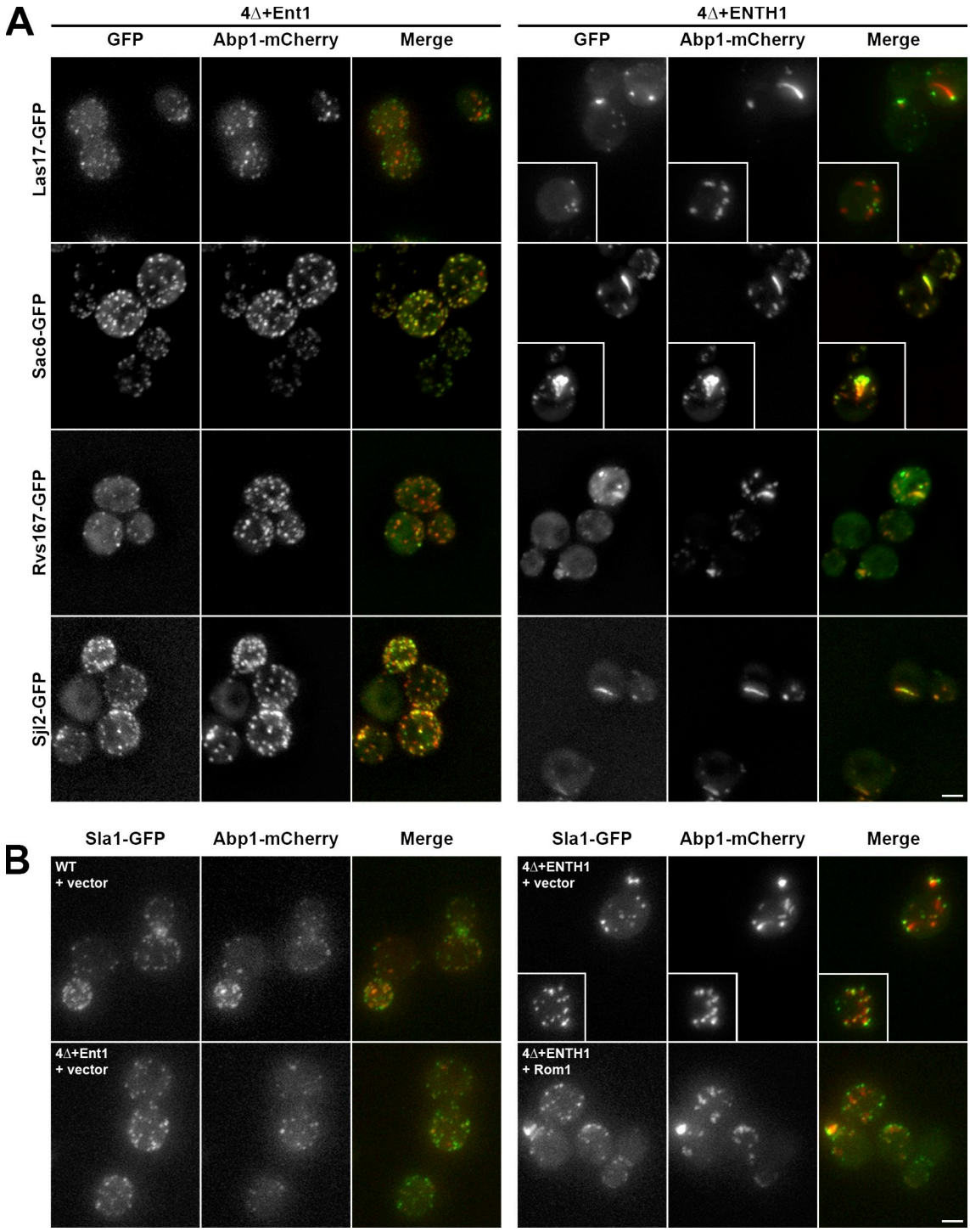

Figure 8. **Accumulation of actin module components in aberrant comet tail structures.** (A) 4Δ+Ent1 and 4Δ+ENTH1 cells expressing GFP-tagged Las17, Sac6, Rvs167, or Sjl2 and Abp1-mCherry were assessed for colocalization of GFP (green) and mCherry (red) signals. Projection images from 0.25-µm-step z stacks are shown. (B) Projection images of WT, 4Δ+Ent1, and 4Δ+ENTH1 strains expressing Sla1-GFP and Abp1-mCherry with empty vector or Rom1 as indicated. Insets show additional cells at the same magnification. Bars, 2.5 µm.

in WT, 4Δ+Ent1, and 4Δ+ENTH1 cells, and asked whether multicopy Rom1 could correct lifetime and/or inward movement defects. We were unable to analyze dynamics of the actin module component Abp1, which appears shortly before inward movement of the actin patch, because of its accumulation in comet tail structures in 4Δ+ENTH1 cells.

The behavior and dynamics of GFP-tagged Ede1, Pan1, and Las17 in WT cells all had lifetimes similar to previously published values (130.8 ± 8.1, 37.0 ± 1.3, and 35.9 ± 1.2 s, respectively; Fig. 9 A; Kaksonen et al., 2003; Kaksonen et al., 2005; Maldonado-Báez et al., 2008; Stimpson et al., 2009). As expected, Pan1 moved inward, whereas Ede1 and Las17, which

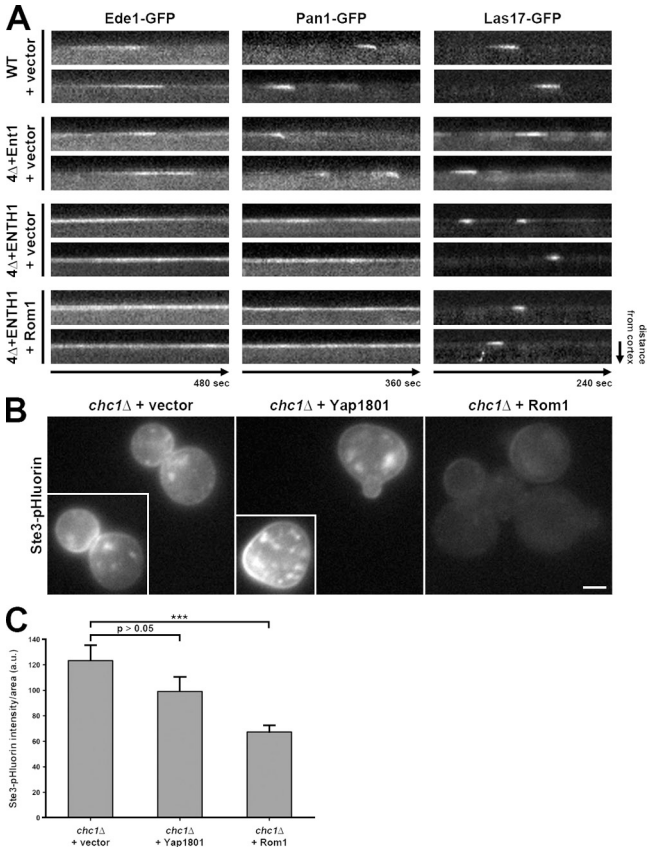

Figure 9. **Rho1-mediated endocytosis does not restore cortical actin patch dynamics, and functions in the absence of clathrin.** (A) Kymograph analysis of WT, 4Δ+Ent1, and 4Δ+ENTH1 cells expressing GFP-tagged Ede1, Pan1, or Las17 with empty vector or Rom1 as indicated. Images were collected every 4 s (480 s total) for Ede1, every 3 s (360 s total) for Pan1, and every 2 s (240 s total) for Las17. (B) Ste3-pHluorin localization was assessed in *chc1*Δ cells with empty vector, Yap1801, or Rom1 as indicated. Insets show additional cells at the same magnification. Bar, 2.5 µm. (C) Quantification of Ste3-pHluorin intensity (a.u.; error bars indicate mean ± SEM; ***, P < 0.001) in cells from B.

both dissociate from the cortical patch before vesicle scission, did not show inward movement. In 4Δ+Ent1 cells, the results were like WT cells for Ede1-GFP and Las17-GFP (128.8 ± 8.2 and 33.8 ± 0.9 s lifetimes, respectively), whereas Pan1-GFP had a modest decrease in lifetime (to 24.8 ± 0.9 s) but still moved inward (Maldonado-Báez et al., 2008). In contrast, 4Δ+ENTH1 cells showed altered dynamics for all three proteins: most Pan1-GFP and Ede1-GFP patches were present over the entire 6- or 8-min observation period, with very few, if any, appearing and dissipating within this time frame. In contrast to Ede1-GFP and Pan1-GFP, the Las17-GFP lifetime was reduced to 19.8 ± 1.0 s in 4Δ+ENTH1 cells; similar Las17-GFP behavior was previously seen in *chc1*Δ cells (Kaksonen et al., 2005). High-copy Rom1 in 4Δ+ENTH1 cells had no effect on the abnormal dynamics of any of these three proteins, with most Pan1-GFP and Ede1-GFP lifetimes of >6 and 8 min, respectively, and Las17-GFP lifetimes of 19.9 ± 0.9 s. These results suggest that defects in lifetime and dynamics of CME machinery at cortical patches are not restored by the Rho1 pathway, even though endocytosis (defined by Ste3 and Mup1 internalization) is improved in these cells. Because Abp1 comet tails emanate from cortical patches that remain aberrant in Rom1-overexpressing 4Δ+ENTH1 cells, these data further suggest that Abp1 comet tails are not productive sites of Rho1-mediated endocytosis.

The Rho1 pathway promotes endocytosis in clathrin-deficient cells

The inability of the Rho1 pathway to restore dynamics of the CME machinery is consistent with observations that endocytosis does not strictly require clathrin (Payne et al., 1988; Chu et al., 1996), and suggests that the Rho1 pathway may mediate CIE. Thus, we asked if Rom1 could promote endocytosis in *chc1*Δ cells lacking the clathrin heavy chain. In addition to retention at the plasma membrane, Ste3-GFP accumulated in numerous, disperse intracellular compartments similar to the previously described distribution of GFP-Snc1 in *clc1*Δ cells (Burston et al., 2009; unpublished data). These structures, which included fragmented vacuolar and nonvacuolar compartments, impeded our analysis of Ste3-GFP localization; instead, we used Ste3-pHluorin, which showed fewer internal fluorescent structures and better allowed us to assess changes in plasma membrane retention of Ste3. In *chc1*Δ cells, Ste3-pHluorin was readily observed at the plasma membrane, whereas this plasma membrane pool was reduced by high-copy Rom1 (Fig. 9, B and C). In contrast, accumulated plasma membrane–localized Ste3-pHluorin or Ste3-GFP was not significantly corrected by high-copy Yap1801, which acts with clathrin to mediate CME (Fig. 9, B and C; and unpublished data). Thus, endocytosis through the Rho1 pathway does not require clathrin.

Osmotic support improves Rho1-mediated endocytosis in adaptor mutant cells

Because Mid2 and its downstream signaling pathways are implicated in osmotic stress responses, we next asked whether osmotic support might facilitate Rho1-mediated endocytosis in 4Δ+ENTH1 cells. We first examined Ste3-GFP localization in WT, 4Δ+Ent1, and 4Δ+ENTH1 cells grown on synthetic medium in the absence or presence of 1 M sorbitol to provide osmotic support. As expected, in the absence of sorbitol, Ste3-GFP was efficiently targeted to the vacuole in WT and 4Δ+Ent1 cells, but was partially retained at the plasma membrane in 4Δ+ENTH1 cells (Figs. 1 C and 10 A). In contrast, addition of sorbitol improved Ste3-GFP internalization and vacuole localization in 4Δ+ENTH1 cells (Fig. 10 A), and did not adversely affect Ste3-GFP localization in WT or 4Δ+Ent1 cells. Thus, osmotic support promotes Ste3-GFP internalization in 4Δ+ENTH1 cells, and multicopy expression of Rho1 pathway components is not required for improved endocytosis.

To ask if the Rho1 pathway contributes to endocytosis in 4Δ+ENTH1 cells grown under osmotic support conditions, we examined the ability of sorbitol to promote endocytosis in 4Δ+ENTH1 cells lacking *BNI1*, *BUD6*, or *TPM1*, which are all required for Rho1-mediated endocytosis in the absence of sorbitol. Addition of sorbitol did not adversely affect Ste3-GFP localization in *bni1*Δ, *bud6*Δ, or *tpm1*Δ WT, or 4Δ+Ent1 adaptor backgrounds; however, sorbitol no longer promoted Ste3-GFP internalization in *bni1*Δ, *bud6*Δ, or *tpm1*Δ 4Δ+ENTH1 cells (Figs. 10 B and S4). In contrast, sorbitol promoted endocytosis

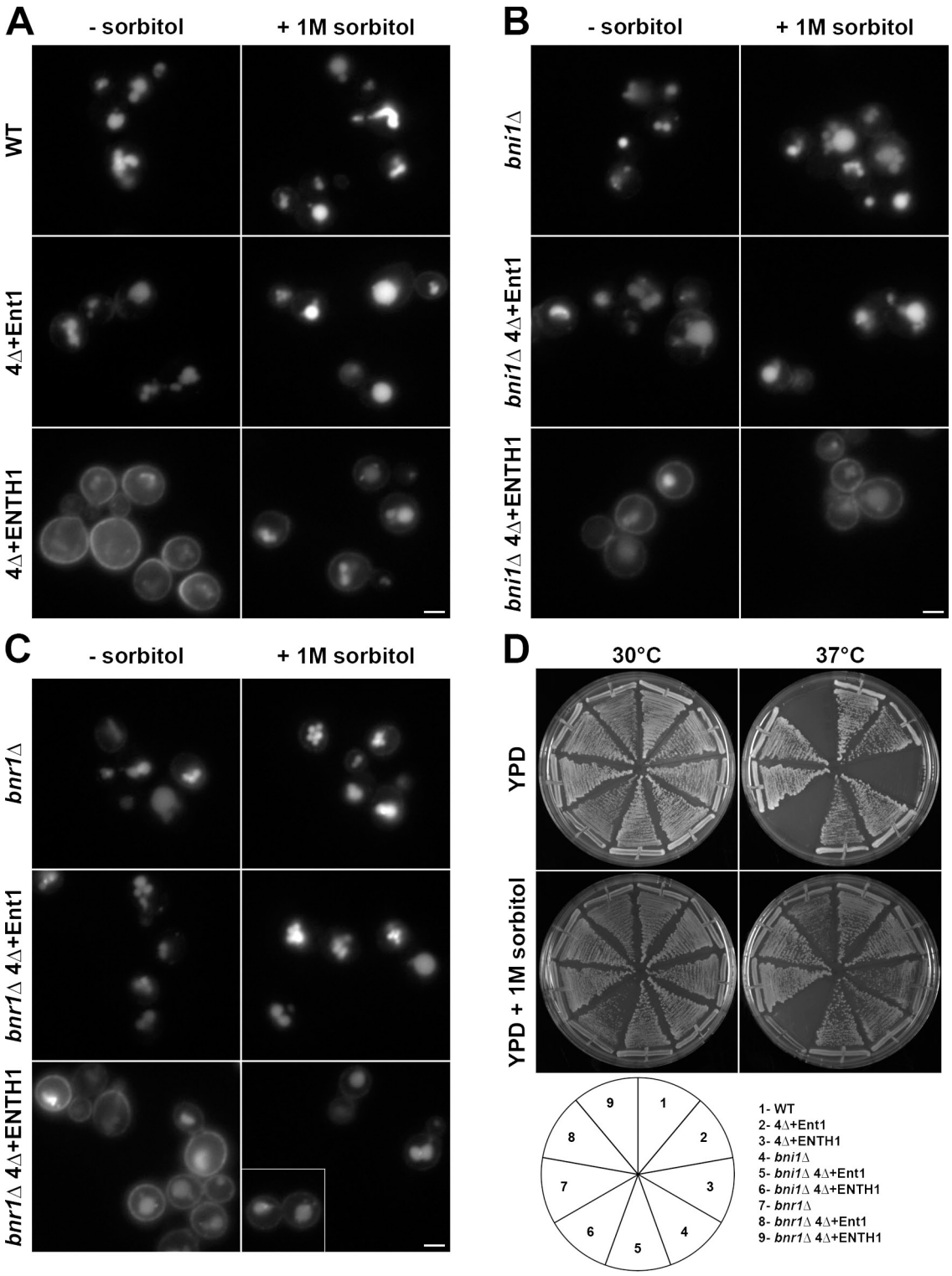

Figure 10. **Bni1-dependent suppression of endocytosis and growth defects in adaptor mutant cells grown with osmotic support.** (A) WT, 4Δ+Ent1, and 4Δ+ENTH1 cells expressing Ste3-GFP were grown on synthetic medium in the absence (−sorbitol) or presence (+ 1 M sorbitol) of osmotic support as indicated and imaged by fluorescence microscopy. *bni1*Δ and *bnr1*Δ (B and C, respectively) in WT, 4Δ+Ent1, and 4Δ+ENTH1 adaptor backgrounds were assessed for Ste3-GFP localization in the absence or presence of osmotic support as in A. The inset shows additional cells at the same magnification. Bars, 2.5 μm. (D) Growth of strains used in A–C at permissive (30°C) and nonpermissive (37°C) temperatures in the absence (YPD) or presence (YPD + 1 M sorbitol) of osmotic support.

of Ste3-GFP in 4Δ+ENTH1 cells lacking *BNR1*, which is not required for Rho1-mediated endocytosis (Fig. 10 C). Of note, addition of 1 M sorbitol also suppressed the temperature sensitivity of 4Δ+ENTH1 and *bnr1*Δ 4Δ+ENTH1 cells, but had little effect on growth of *bni1*Δ 4Δ+ENTH1 cells at 37°C (Fig. 10 D). These data indicate that proteins involved in

the Rho1 pathway are required for improved endocytosis in 4Δ+ENTH1 cells under osmotic support conditions, and that the ability to promote endocytosis is not solely caused by overexpression of Rho1 pathway components.

Discussion

Considering the variety of CIE mechanisms in most eukaryotes, the apparent lack of CIE in yeast has remained a long-standing puzzle. Although clathrin itself is not essential for endocytosis in yeast, CME machinery has been proposed to contribute to residual endocytosis in clathrin-null cells (Kaksonen et al., 2005; Newpher and Lemmon, 2006). Here, we present what is to our knowledge the first evidence of an endocytic pathway distinct from the well-studied yeast CME pathway. The Rho1-dependent pathway does not require clathrin, adaptor proteins, robust Arp2/3-mediated actin polymerization, or actin bundlers (Sac6 and Scp1), all of which are key elements of CME in yeast and mammalian cells (Kaksonen et al., 2006; Robertson et al., 2009). Instead, this alternative pathway acts through Rho1 and the formin Bni1, which mediates the formation of actin cables. Although the Rho1 pathway is unlikely to fully account for residual endocytosis in adaptor-deficient cells, our study provides evidence of a direct role for formins in endocytosis; it will be interesting to see if formins similarly contribute to endocytosis in other cell types.

Comparison of the Rho1 pathway with established endocytic routes

Rho1 regulates CWI, but has also been implicated in endocytosis in yeast (deHart et al., 2003). Notably, several key differences between our study and the deHart et al. (2003) study indicate that our Rho1-mediated pathway constitutes a distinct endocytic route. In particular, the Rho1 pathway described by deHart et al. (2003) requires Wsc1, Rom2, and Fks1, but not Mid2, Rom1, or Bni1, and acts downstream of Tor2 in cells with intact CME machinery. In contrast, our Rho1 pathway acts through Mid2, Rom1/2, Bni1, and Skn7, but not Wsc1 or Fks1. Fks1 interaction with CME machinery components (Gavin et al., 2002) suggests that the previously described role for Rho1 in endocytosis could be through modulating CME; such a function does not preclude additional roles for Rho1 in CIE.

RhoA, the mammalian orthologue of yeast Rho1, functions in CIE of cargos such as the IL2 interleukin receptor (Lamaze et al., 2001). The GTPase dynamin is the only other protein known to contribute to RhoA endocytic function. Intriguingly, our preliminary results suggest an essential function for the dynamin-like protein Vps1 in 4Δ+ENTH1 cells (unpublished data). RhoA and dynamin also contribute to phagocytosis, as do mammalian integrins and formins (Gold et al., 1999; Werner et al., 2001; Seth et al., 2006; Brandt et al., 2007). Mid2 is topologically similar to integrins, bearing a heavily glycosylated N-terminal extracellular domain and a short cytoplasmic C terminus that mediates signaling. Thus, the yeast Rho1 pathway has similarities to mammalian RhoA-mediated endocytosis; it will be interesting to determine whether the Rho1 pathway more closely resembles RhoA-dependent CIE or phagocytosis.

Although the polarisome is not conserved in mammals, localized recruitment and concentration of factors that regulate membrane remodeling is likely a common theme in endocytosis. In mammalian cells, integrins, RhoA, and formins become polarized during cell migration (Vicente-Manzanares et al., 2003; Francis et al., 2006), which suggests that mammalian polarity cues concentrate actin and membrane remodeling factors to discrete plasma membrane sites. Similarly, localized recruitment of these mammalian proteins is likely critical for their established roles in CIE.

Distinctions between the Rho1 and CME pathways

How might the Rho1 pathway promote endocytosis in CME-deficient cells? First, Rho1 pathway activation might favor maturation of defective cortical actin patches into productive endocytic sites, but this seems unlikely because high-copy Rom1 did not restore dynamics of cortical patch proteins. Second, the Rho1 pathway might facilitate cargo recruitment into defective CME sites that internalize at reduced rates. Again, this seems unlikely because cortical patch dynamics and morphology remain aberrant. Cargo enrichment is thought to play a role in progression of CME sites and completion of endocytosis (Ehrlich et al., 2004; Loerke et al., 2009; Layton et al., 2011). *chc1*Δ cells accumulate the membrane dye FM4-64 in comet tails that eventually internalize (Newpher and Lemmon, 2006); however, incorporation of protein cargo into comet tails has not been demonstrated. Similar to *chc1*Δ cells, 4Δ+ENTH1 cells are likely deficient in cargo enrichment at CME sites, resulting in aberrant Ede1 and Pan1 cortical patch dynamics. Consistent with defective protein cargo recruitment, we did not observe Ste3-GFP enrichment in comet tail structures in either 4Δ+ENTH1 or *chc1*Δ cells.

The Rho1 pathway is unlikely to entirely account for residual endocytosis in CME mutant strains, as deletion of *BNI1*, *TPM1*, *BUD6*, and *SPA2*, which are key components of the Rho1 pathway, does not abolish vacuolar Ste3-GFP in 4Δ+ENTH1 cells. We suggest that the Rho1 pathway promotes endocytosis in CME-deficient cells independent of the CME machinery because Bni1 and actin cables are not implicated in CME and are not known to localize to cortical actin patches. Interestingly, Arp2/3 is not absolutely required for endocytosis in *Candida albicans*, although the role of other CME components in *C. albicans* is not clear (Epp et al., 2010).

Another possibility is that the Rho1 pathway acts at eisosomes, which are plasma membrane–associated structures suggested to form static sites of endocytosis (Walther et al., 2006). However, the role of eisosomes in endocytosis is controversial, and recent evidence suggests that they do not significantly contribute to cargo internalization (Grossmann et al., 2008; Strádalová et al., 2009; Brach et al., 2011). Whether or not eisosomes correspond to endocytic sites, the Rho1 pathway is unlikely to act through eisosomes because multicopy Rom1 promotes endocytosis in 4Δ+ENTH1 cells lacking *PIL1*, the principal structural component required for eisosome formation and maintenance (unpublished data).

Possible mechanisms and roles for the Rho1 endocytic pathway

Although the sites of Rho1-mediated endocytosis are unclear, Bni1 localization at polarisome sites at the cell cortex is of particular interest, including tips of budding cells and bud necks in large-budded cells. For Rho1-mediated endocytosis, the polarisome might serve as a site of localized Bni1 recruitment and activation, and subsequent actin assembly could provide the forces needed for membrane deformation independent of Arp2/3. Interestingly, Bni1 localizes to cytoplasmic punctae (Buttery et al., 2007), and has also been observed at highly dynamic cortical patches that are distinct from CME sites (Yu et al., 2011). Future studies will reveal whether other polarisome components involved in the Rho1 pathway such as Spa2 and Bud6 show similar dynamic behavior, and whether these newly-identified Bni1 patches correspond to CIE sites. Other possible mechanisms for Rho1-mediated endocytosis include, but are not limited to, consumption by preexisting endosomes moving along actin cables (Toshima et al., 2006) and force generation by actin cable–linked motor proteins such as Myo2 or Myo4.

A key unresolved issue is how the Rho1 pathway contributes to endocytosis in cells with intact CME machinery. Bni1 and actin cables are required for the Rho1 pathway, as are the polarisome components Spa2 and Bud6. However, *bni1*Δ cells have no obvious endocytic defects when the CME machinery is intact (Sagot et al., 2002; deHart et al., 2003); CME is likely the predominant endocytic route under standard laboratory conditions. The Rho1 pathway might instead be required for internalization of specific cargos that do not normally enter through CME, whereas Rho1 pathway up-regulation in endocytic mutant cells could promote more generalized cargo internalization, including CME cargo. Alternatively, the Rho1 pathway might be activated by specific stresses such as osmotic stress and cell wall or plasma membrane damage, and could aid rapid internalization of damaged components. To date, all well-studied endocytic cargos in yeast enter through the CME pathway. The CME machinery may be maximally efficient at internalizing such cargos, making it difficult to accurately determine the relative contribution of the Rho1 pathway to endocytosis in WT cells under laboratory conditions. Our future studies will be directed toward identifying cargos that normally enter through the Rho1 pathway, discovering whether specific stress conditions stimulate Rho1-mediated endocytosis, and precisely defining the machinery and dynamics of the Rho1 pathway.

Materials and methods

Strains and plasmids

Strains and plasmids used in this study are described in Tables S1 and S2, respectively. The pWSC1 plasmid was provided by D. Levin (Boston University, Boston, MA); pPKC1, pPKC1*, pBCK1-20, pMKK1, pMPK1, pBNI1, pFKS1, and pSKN7 were from M. Hall (University of Basel, Basel, Switzerland); pNRB807 was from W. Guo (University of Pennsylvania, Philadelphia, PA); pBNI1.314, pBNI1-FΔA.314, pBNI1-FΔB.314, pBNI1-FΔC.314, and pBNI1-FΔD.314 were from Y. Takai (Kobe University, Kobe, Japan). Strains were constructed using PCR-based genomic integration as described previously (Longtine et al., 1998; Goldstein and McCusker, 1999). All cells were grown in rich (yeast peptone dextrose [YPD]) medium or in synthetic (yeast nitrogen base [YNB]) medium lacking uracil, tryptophan, or lysine to maintain specific plasmids. For osmotic support experiments, cells were grown overnight on media supplemented with 1 M sorbitol before imaging.

High-copy suppressor screen

We screened 4Δ+ENTH1 cells for genes that promoted endocytosis by transformation with a genomic DNA library cloned into the high-copy YEp24 backbone (Carlson and Botstein, 1982). Transformed cells were plated onto YNB −ura medium overnight at 30°C, followed by replica plating onto YNB −ura at 37°C. Plasmid dependence of growth at 37°C was confirmed by selection for plasmid loss on 5-fluoroorotic acid (5-FOA; Sigma-Aldrich) followed by growth at 37°C on YNB −Trp. Plasmids were isolated from the original transformant colonies for insert sequencing. A total of 4,084 transformants were screened, yielding nine unique clones.

Microscopy and image analysis

Images were acquired using either an inverted microscope (Axiovert 200; Carl Zeiss) equipped with a Sensicam (Cooke), an X-Cite 120 PC fluorescence illumination system, and a 100×, 1.4 NA Plan-Apochromat objective lens, or with a microscope (Marianas; 3i) equipped with a α-Plan-Fluor 100× 1.45 NA objective lens (Carl Zeiss), EM cameras (Cascade II 512; Photometrics), a 488-nm diode laser, and SlideBook 4.2 software (3i). All imaging was performed at room temperature in YNB medium unless otherwise noted, and identical acquisition parameters were used for all samples within an experiment. Image analysis was performed using ImageJ v1.41n (National Institutes of Health, http://rsb.info.nih.gov/ij/). For all Ste3-GFP images, identical maximum and minimum intensity values were applied to each sample within a set of WT, 4Δ+Ent1, and 4Δ+ENTH1 cells to allow comparison of relative Ste3-GFP distribution. Kymographs were generated using the multiple kymograph plugin (http://www.embl-heidelberg.de/eamnet/html/kymograph.html).

For projection images, z stacks were collected at 0.25-µm step intervals over a 6.25-µm distance. Maximum intensity projections were generated using SlideBook 4.2.

Quantification of Ste3-pHluorin fluorescence intensity

We quantified whole-cell Ste3-pHluorin fluorescence intensity as described previously (Prosser et al., 2010). In brief, images were collected using identical image acquisition parameters for all images in the experiment. Integrated density was measured from background-subtracted 16-bit images using ImageJ, and values were corrected for cell size.

Mup1-pHluorin internalization assay

To accumulate Mup1-pHluorin at the plasma membrane, cells were grown overnight in YNB −ura −Met medium. Cultures were then diluted in YNB −ura −Met and grown to mid-logarithmic phase before seeding onto 8-well chamber slides (Labtek) coated with Concanavalin A. Random fields of cells were imaged before or 30 min after addition of methionine to a final concentration 20 µg/ml, and cells were maintained at a constant temperature of 30°C. Whole-cell fluorescence intensity was quantified as described above for Ste3-pHluorin.

LatA treatment

For actin depolymerization experiments, cells grown in synthetic medium were pelleted at 1,500 *g*, and were then resuspended in synthetic medium containing 200 µM LatA (Invitrogen) or an equivalent volume of DMSO. Cells were incubated for 2 h at 30°C before imaging to allow plasma membrane accumulation of Ste3-GFP.

Statistical analysis

For all quantitative experiments, fluorescence intensity was analyzed for a minimum of 35 cells. Statistical significance between populations was determined by one-way ANOVA followed by Tukey's Multiple Comparison post hoc analysis.

Online supplemental material

Fig. S1 shows that up-regulation of the Rho1 pathway does not bypass the requirement for an ENTH domain in 4Δ cells. Fig. S2 shows the effect of Rho1 effector overexpression or activation on Rho1-mediated endocytosis. Fig. S3 shows quantification of Mup1-pHluorin internalization in *bni1*Δ and *bnr1*Δ strains. Fig. S4 shows the effect of osmotic support on Ste3-GFP localization in *bud6*Δ and *tpm1*Δ strains. Tables S1 and S2 show strains and plasmids used in this study, respectively. Online supplemental material is available at http://www.jcb.org/cgi/content/full/jcb.201104045/DC1.

We thank Wei Guo (University of Pennsylvania), Michael Hall (University of Basel, Switzerland), David Levin (Boston University), Hay-Oak Park

(Ohio State University), and Yoshimi Takai (Kobe University, Japan) for plasmids used in this study; Nathan Wright for technical assistance; Boonsom Uranukul, Kristie Wrasman, Kirstie Keller, Karen Whitworth, and Robert Sershon for help with strains and plasmids. We also acknowledge The Johns Hopkins University Integrated Imaging Center for its excellent resources and expertise of Michael McCaffery and Erin Pryce. We are grateful to Chris Burd and Sandra Lemmon for helpful discussions and to Julie Donaldson, Bruce Goode, and members of the Wendland laboratory for helpful discussions and comments on the manuscript.

This work was supported by grants from the National Institutes of Health (to B. Wendland, NIH RO1 GM60979) and the National Science Foundation (to B. Wendland, MCB 1024818).

Submitted: 11 April 2011
Accepted: 12 October 2011

References

Aghamohammadzadeh, S., and K.R. Ayscough. 2009. Differential requirements for actin during yeast and mammalian endocytosis. *Nat. Cell Biol.* 11:1039–1042. doi:10.1038/ncb1918

Aguilar, R.C., H.A. Watson, and B. Wendland. 2003. The yeast Epsin Ent1 is recruited to membranes through multiple independent interactions. *J. Biol. Chem.* 278:10737–10743. doi:10.1074/jbc.M211622200

Aguilar, R.C., S.A. Longhi, J.D. Shaw, L.Y. Yeh, S. Kim, A. Schön, E. Freire, A. Hsu, W.K. McCormick, H.A. Watson, and B. Wendland. 2006. Epsin N-terminal homology domains perform an essential function regulating Cdc42 through binding Cdc42 GTPase-activating proteins. *Proc. Natl. Acad. Sci. USA*. 103:4116–4121. doi:10.1073/pnas.0510513103

Alberts, A.S. 2001. Identification of a carboxyl-terminal diaphanous-related formin homology protein autoregulatory domain. *J. Biol. Chem.* 276:2824–2830. doi:10.1074/jbc.M006205200

Ayscough, K.R., J. Stryker, N. Pokala, M. Sanders, P. Crews, and D.G. Drubin. 1997. High rates of actin filament turnover in budding yeast and roles for actin in establishment and maintenance of cell polarity revealed using the actin inhibitor latrunculin-A. *J. Cell Biol.* 137:399–416. doi:10.1083/jcb.137.2.399

Brach, T., T. Specht, and M. Kaksonen. 2011. Reassessment of the role of plasma membrane domains in the regulation of vesicular traffic in yeast. *J. Cell Sci.* 124:328–337. doi:10.1242/jcs.078519

Brandt, D.T., S. Marion, G. Griffiths, T. Watanabe, K. Kaibuchi, and R. Grosse. 2007. Dia1 and IQGAP1 interact in cell migration and phagocytic cup formation. *J. Cell Biol.* 178:193–200. doi:10.1083/jcb.200612071

Burston, H.E., L. Maldonado-Báez, M. Davey, B. Montpetit, C. Schluter, B. Wendland, and E. Conibear. 2009. Regulators of yeast endocytosis identified by systematic quantitative analysis. *J. Cell Biol.* 185:1097–1110. doi:10.1083/jcb.200811116

Buttery, S.M., S. Yoshida, and D. Pellman. 2007. Yeast formins Bni1 and Bnr1 utilize different modes of cortical interaction during the assembly of actin cables. *Mol. Biol. Cell*. 18:1826–1838. doi:10.1091/mbc.E06-09-0820

Carlson, M., and D. Botstein. 1982. Two differentially regulated mRNAs with different 5′ ends encode secreted with intracellular forms of yeast invertase. *Cell*. 28:145–154. doi:10.1016/0092-8674(82)90384-1

Chu, D.S., B. Pishvaee, and G.S. Payne. 1996. The light chain subunit is required for clathrin function in *Saccharomyces cerevisiae*. *J. Biol. Chem.* 271:33123–33130. doi:10.1074/jbc.271.51.33123

deHart, A.K., J.D. Schnell, D.A. Allen, J.Y. Tsai, and L. Hicke. 2003. Receptor internalization in yeast requires the Tor2-Rho1 signaling pathway. *Mol. Biol. Cell*. 14:4676–4684. doi:10.1091/mbc.E03-05-0323

Delley, P.A., and M.N. Hall. 1999. Cell wall stress depolarizes cell growth via hyperactivation of RHO1. *J. Cell Biol.* 147:163–174. doi:10.1083/jcb.147.1.163

Drees, B., C. Brown, B.G. Barrell, and A. Bretscher. 1995. Tropomyosin is essential in yeast, yet the TPM1 and TPM2 products perform distinct functions. *J. Cell Biol.* 128:383–392. doi:10.1083/jcb.128.3.383

Ehrlich, M., W. Boll, A. Van Oijen, R. Hariharan, K. Chandran, M.L. Nibert, and T. Kirchhausen. 2004. Endocytosis by random initiation and stabilization of clathrin-coated pits. *Cell*. 118:591–605. doi:10.1016/j.cell.2004.08.017

Engqvist-Goldstein, A.E., and D.G. Drubin. 2003. Actin assembly and endocytosis: from yeast to mammals. *Annu. Rev. Cell Dev. Biol.* 19:287–332. doi:10.1146/annurev.cellbio.19.111401.093127

Epp, E., A. Walther, G. Lépine, Z. Leon, A. Mullick, M. Raymond, J. Wendland, and M. Whiteway. 2010. Forward genetics in *Candida albicans* that reveals the Arp2/3 complex is required for hyphal formation, but not endocytosis. *Mol. Microbiol.* 75:1182–1198. doi:10.1111/j.1365-2958.2009.07038.x

Evangelista, M., K. Blundell, M.S. Longtine, C.J. Chow, N. Adames, J.R. Pringle, M. Peter, and C. Boone. 1997. Bni1p, a yeast formin linking cdc42p and the actin cytoskeleton during polarized morphogenesis. *Science*. 276:118–122. doi:10.1126/science.276.5309.118

Evangelista, M., D. Pruyne, D.C. Amberg, C. Boone, and A. Bretscher. 2002. Formins direct Arp2/3-independent actin filament assembly to polarize cell growth in yeast. *Nat. Cell Biol.* 4:260–269.

Francis, S.A., X. Shen, J.B. Young, P. Kaul, and D.J. Lerner. 2006. Rho GEF Lsc is required for normal polarization, migration, and adhesion of formyl-peptide-stimulated neutrophils. *Blood*. 107:1627–1635. doi:10.1182/blood-2005-03-1164

Fujiwara, T., K. Tanaka, A. Mino, M. Kikyo, K. Takahashi, K. Shimizu, and Y. Takai. 1998. Rho1p-Bni1p-Spa2p interactions: implication in localization of Bni1p at the bud site and regulation of the actin cytoskeleton in *Saccharomyces cerevisiae*. *Mol. Biol. Cell*. 9:1221–1233.

Gavin, A.C., M. Bösche, R. Krause, P. Grandi, M. Marzioch, A. Bauer, J. Schultz, J.M. Rick, A.M. Michon, C.M. Cruciat, et al. 2002. Functional organization of the yeast proteome by systematic analysis of protein complexes. *Nature*. 415:141–147. doi:10.1038/415141a

Gold, E.S., D.M. Underhill, N.S. Morrissette, J. Guo, M.A. McNiven, and A. Aderem. 1999. Dynamin 2 is required for phagocytosis in macrophages. *J. Exp. Med.* 190:1849–1856. doi:10.1084/jem.190.12.1849

Goldstein, A.L., and J.H. McCusker. 1999. Three new dominant drug resistance cassettes for gene disruption in *Saccharomyces cerevisiae*. *Yeast*. 15:1541–1553. doi:10.1002/(SICI)1097-0061(199910)15:14<1541::AID-YEA476>3.0.CO;2-K

Goodman, A., B.L. Goode, P. Matsudaira, and G.R. Fink. 2003. The *Saccharomyces cerevisiae* calponin/transgelin homolog Scp1 functions with fimbrin to regulate stability and organization of the actin cytoskeleton. *Mol. Biol. Cell*. 14:2617–2629. doi:10.1091/mbc.E03-01-0028

Grossmann, G., J. Malinsky, W. Stahlschmidt, M. Loibl, I. Weig-Meckl, W.B. Frommer, M. Opekarová, and W. Tanner. 2008. Plasma membrane microdomains regulate turnover of transport proteins in yeast. *J. Cell Biol.* 183:1075–1088. doi:10.1083/jcb.200806035

Howes, M.T., S. Mayor, and R.G. Parton. 2010. Molecules, mechanisms, and cellular roles of clathrin-independent endocytosis. *Curr. Opin. Cell Biol.* 22:519–527. doi:10.1016/j.ceb.2010.04.001

Huang, C., and A. Chang. 2011. pH-dependent cargo sorting from the Golgi. *J. Biol. Chem.* 286:10058–10065. doi:10.1074/jbc.M110.197889

Imamura, H., K. Tanaka, T. Hihara, M. Umikawa, T. Kamei, K. Takahashi, T. Sasaki, and Y. Takai. 1997. Bni1p and Bnr1p: downstream targets of the Rho family small G-proteins which interact with profilin and regulate actin cytoskeleton in *Saccharomyces cerevisiae*. *EMBO J.* 16:2745–2755. doi:10.1093/emboj/16.10.2745

Kaksonen, M., Y. Sun, and D.G. Drubin. 2003. A pathway for association of receptors, adaptors, and actin during endocytic internalization. *Cell*. 115:475–487. doi:10.1016/S0092-8674(03)00883-3

Kaksonen, M., C.P. Toret, and D.G. Drubin. 2005. A modular design for the clathrin- and actin-mediated endocytosis machinery. *Cell*. 123:305–320. doi:10.1016/j.cell.2005.09.024

Kaksonen, M., C.P. Toret, and D.G. Drubin. 2006. Harnessing actin dynamics for clathrin-mediated endocytosis. *Nat. Rev. Mol. Cell Biol.* 7:404–414. doi:10.1038/nrm1940

Kiss, A.L., and E. Botos. 2009. Endocytosis via caveolae: alternative pathway with distinct cellular compartments to avoid lysosomal degradation? *J. Cell. Mol. Med.* 13:1228–1237. doi:10.1111/j.1582-4934.2009.00754.x

Lamaze, C., A. Dujeancourt, T. Baba, C.G. Lo, A. Benmerah, and A. Dautry-Varsat. 2001. Interleukin 2 receptors and detergent-resistant membrane domains define a clathrin-independent endocytic pathway. *Mol. Cell*. 7:661–671. doi:10.1016/S1097-2765(01)00212-X

Layton, A.T., N.S. Savage, A.S. Howell, S.Y. Carroll, D.G. Drubin, and D.J. Lew. 2011. Modeling vesicle traffic reveals unexpected consequences for Cdc42p-mediated polarity establishment. *Curr. Biol.* 21:184–194. doi:10.1016/j.cub.2011.01.012

Lee, K.S., and D.E. Levin. 1992. Dominant mutations in a gene encoding a putative protein kinase (BCK1) bypass the requirement for a *Saccharomyces cerevisiae* protein kinase C homolog. *Mol. Cell. Biol.* 12:172–182.

Levin, D.E. 2005. Cell wall integrity signaling in *Saccharomyces cerevisiae*. *Microbiol. Mol. Biol. Rev.* 69:262–291. doi:10.1128/MMBR.69.2.262-291.2005

Levin, D.E., and E. Bartlett-Heubusch. 1992. Mutants in the *S. cerevisiae* PKC1 gene display a cell cycle-specific osmotic stability defect. *J. Cell Biol.* 116:1221–1229. doi:10.1083/jcb.116.5.1221

Liu, H.P., and A. Bretscher. 1989. Disruption of the single tropomyosin gene in yeast results in the disappearance of actin cables from the cytoskeleton. *Cell*. 57:233–242. doi:10.1016/0092-8674(89)90961-6

Loerke, D., M. Mettlen, D. Yarar, K. Jaqaman, H. Jaqaman, G. Danuser, and S.L. Schmid. 2009. Cargo and dynamin regulate clathrin-coated pit maturation. *PLoS Biol.* 7:e57. doi:10.1371/journal.pbio.1000057

Longtine, M.S., A. McKenzie III, D.J. Demarini, N.G. Shah, A. Wach, A. Brachat, P. Philippsen, and J.R. Pringle. 1998. Additional modules for versatile and economical PCR-based gene deletion and modification in Saccharomyces cerevisiae. *Yeast*. 14:953–961. doi:10.1002/(SICI)1097-0061(199807)14:10<953::AID-YEA293>3.0.CO;2-U

Madania, A., P. Dumoulin, S. Grava, H. Kitamoto, C. Schärer-Brodbeck, A. Soulard, V. Moreau, and B. Winsor. 1999. The *Saccharomyces cerevisiae* homologue of human Wiskott-Aldrich syndrome protein Las17p interacts with the Arp2/3 complex. *Mol. Biol. Cell*. 10:3521–3538.

Maldonado-Báez, L., M.R. Dores, E.M. Perkins, T.G. Drivas, L. Hicke, and B. Wendland. 2008. Interaction between Epsin/Yap180 adaptors and the scaffolds Ede1/Pan1 is required for endocytosis. *Mol. Biol. Cell*. 19:2936–2948. doi:10.1091/mbc.E07-10-1019

Mayor, S., and R.E. Pagano. 2007. Pathways of clathrin-independent endocytosis. *Nat. Rev. Mol. Cell Biol.* 8:603–612. doi:10.1038/nrm2216

Mazzoni, C., P. Zarov, A. Rambourg, and C. Mann. 1993. The SLT2 (MPK1) MAP kinase homolog is involved in polarized cell growth in *Saccharomyces cerevisiae. J. Cell Biol.* 123:1821–1833. doi:10.1083/jcb.123.6.1821

Miesenböck, G., D.A. De Angelis, and J.E. Rothman. 1998. Visualizing secretion and synaptic transmission with pH-sensitive green fluorescent proteins. *Nature*. 394:192–195. doi:10.1038/28190

Moseley, J.B., I. Sagot, A.L. Manning, Y. Xu, M.J. Eck, D. Pellman, and B.L. Goode. 2004. A conserved mechanism for Bni1- and mDia1-induced actin assembly and dual regulation of Bni1 by Bud6 and profilin. *Mol. Biol. Cell*. 15:896–907. doi:10.1091/mbc.E03-08-0621

Newpher, T.M., and S.K. Lemmon. 2006. Clathrin is important for normal actin dynamics and progression of Sla2p-containing patches during endocytosis in yeast. *Traffic*. 7:574–588. doi:10.1111/j.1600-0854.2006.00410.x

Ozaki-Kuroda, K., Y. Yamamoto, H. Nohara, M. Kinoshita, T. Fujiwara, K. Irie, and Y. Takai. 2001. Dynamic localization and function of Bni1p at the sites of directed growth in *Saccharomyces cerevisiae. Mol. Cell. Biol.* 21:827–839. doi:10.1128/MCB.21.3.827-839.2001

Payne, G.S., D. Baker, E. van Tuinen, and R. Schekman. 1988. Protein transport to the vacuole and receptor-mediated endocytosis by clathrin heavy chain-deficient yeast. *J. Cell Biol.* 106:1453–1461. doi:10.1083/jcb.106.5.1453

Philip, B., and D.E. Levin. 2001. Wsc1 and Mid2 are cell surface sensors for cell wall integrity signaling that act through Rom2, a guanine nucleotide exchange factor for Rho1. *Mol. Cell. Biol.* 21:271–280. doi:10.1128/MCB.21.1.271-280.2001

Prosser, D.C., K. Whitworth, and B. Wendland. 2010. Quantitative analysis of endocytosis with cytoplasmic pHluorin chimeras. *Traffic*. 11:1141–1150. doi:10.1111/j.1600-0854.2010.01088.x

Pruyne, D., L. Gao, E. Bi, and A. Bretscher. 2004. Stable and dynamic axes of polarity use distinct formin isoforms in budding yeast. *Mol. Biol. Cell*. 15:4971–4989. doi:10.1091/mbc.E04-04-0296

Radhakrishna, H., and J.G. Donaldson. 1997. ADP-ribosylation factor 6 regulates a novel plasma membrane recycling pathway. *J. Cell Biol.* 139:49–61. doi:10.1083/jcb.139.1.49

Robertson, A.S., E. Smythe, and K.R. Ayscough. 2009. Functions of actin in endocytosis. *Cell. Mol. Life Sci.* 66:2049–2065. doi:10.1007/s00018-009-0001-y

Sabharanjak, S., P. Sharma, R.G. Parton, and S. Mayor. 2002. GPI-anchored proteins are delivered to recycling endosomes via a distinct cdc42-regulated, clathrin-independent pinocytic pathway. *Dev. Cell*. 2:411–423. doi:10.1016/S1534-5807(02)00145-4

Sagot, I., S.K. Klee, and D. Pellman. 2002. Yeast formins regulate cell polarity by controlling the assembly of actin cables. *Nat. Cell Biol.* 4:42–50.

Sankaranarayanan, S., D. De Angelis, J.E. Rothman, and T.A. Ryan. 2000. The use of pHluorins for optical measurements of presynaptic activity. *Biophys. J.* 79:2199–2208. doi:10.1016/S0006-3495(00)76468-X

Seth, A., C. Otomo, and M.K. Rosen. 2006. Autoinhibition regulates cellular localization and actin assembly activity of the diaphanous-related formins FRLalpha and mDia1. *J. Cell Biol.* 174:701–713. doi:10.1083/jcb.200605006

Shaw, J.D., H. Hama, F. Sohrabi, D.B. DeWald, and B. Wendland. 2003. PtdIns(3,5)P2 is required for delivery of endocytic cargo into the multivesicular body. *Traffic*. 4:479–490. doi:10.1034/j.1600-0854.2003.t01-1-00106.x

Sheu, Y.J., B. Santos, N. Fortin, C. Costigan, and M. Snyder. 1998. Spa2p interacts with cell polarity proteins and signaling components involved in yeast cell morphogenesis. *Mol. Cell. Biol.* 18:4053–4069.

Stimpson, H.E., C.P. Toret, A.T. Cheng, B.S. Pauly, and D.G. Drubin. 2009. Early-arriving Syp1p and Ede1p function in endocytic site placement and formation in budding yeast. *Mol. Biol. Cell*. 20:4640–4651. doi:10.1091/mbc.E09-05-0429

Strádalová, V., W. Stahlschmidt, G. Grossmann, M. Blazíková, R. Rachel, W. Tanner, and J. Malinsky. 2009. Furrow-like invaginations of the yeast plasma membrane correspond to membrane compartment of Can1. *J. Cell Sci.* 122:2887–2894. doi:10.1242/jcs.051227

Sun, Y., A.C. Martin, and D.G. Drubin. 2006. Endocytic internalization in budding yeast requires coordinated actin nucleation and myosin motor activity. *Dev. Cell*. 11:33–46. doi:10.1016/j.devcel.2006.05.008

Toshima, J.Y., J. Toshima, M. Kaksonen, A.C. Martin, D.S. King, and D.G. Drubin. 2006. Spatial dynamics of receptor-mediated endocytic trafficking in budding yeast revealed by using fluorescent alpha-factor derivatives. *Proc. Natl. Acad. Sci. USA*. 103:5793–5798. doi:10.1073/pnas.0601042103

Vicente-Manzanares, M., M. Rey, M. Pérez-Martínez, M. Yáñez-Mó, D. Sancho, J.R. Cabrero, O. Barreiro, H. de la Fuente, K. Itoh, and F. Sánchez-Madrid. 2003. The RhoA effector mDia is induced during T cell activation and regulates actin polymerization and cell migration in T lymphocytes. *J. Immunol.* 171:1023–1034.

Walther, T.C., J.H. Brickner, P.S. Aguilar, S. Bernales, C. Pantoja, and P. Walter. 2006. Eisosomes mark static sites of endocytosis. *Nature*. 439:998–1003. doi:10.1038/nature04472

Wendland, B., K.E. Steece, and S.D. Emr. 1999. Yeast epsins contain an essential N-terminal ENTH domain, bind clathrin and are required for endocytosis. *EMBO J.* 18:4383–4393. doi:10.1093/emboj/18.16.4383

Werner, E., F. Kheradmand, R.R. Isberg, and Z. Werb. 2001. Phagocytosis mediated by *Yersinia* invasin induces collagenase-1 expression in rabbit synovial fibroblasts through a proinflammatory cascade. *J. Cell Sci.* 114:3333–3343.

Winder, S.J., T. Jess, and K.R. Ayscough. 2003. SCP1 encodes an actin-bundling protein in yeast. *Biochem. J.* 375:287–295. doi:10.1042/BJ20030796

Yu, J.H., A.H. Crevenna, M. Bettenbühl, T. Freisinger, and R. Wedlich-Söldner. 2011. Cortical actin dynamics driven by formins and myosin V. *J. Cell Sci.* 124:1533–1541. doi:10.1242/jcs.079038